Articletype: Annalen der Physik

Light-Switching-Light Optical Transistor based on Metallic Nanoparticle Cross-chains Geometry Incorporating Kerr Nonlinearity

Fathi AbdelMalek[1], Walid Aroua[1], Shyqyri Haxha[2,] and Ian Flint[3]*

*Corresponding Author: E-mail: shyqyri.haxha@beds.ac.uk

[1]National Institute of Applied Science and Technology, BP-676, 1080, Tunis, Tunisia
[2]Computer Science and Technology Department, Bedfordshire University, Luton, United Kingdom
[3]Selex ES Ltd Luton, 300 Capability Green, Luton, Bedfordshire LU1 3PG, United Kingdom

Abstract: In this research work, we propose all-optical transistor based on metallic nanoparticle cross-chains geometry. The geometry of the proposed device consists of two silver nanoparticle chains arranged along the *x*- and *z*-axis. The *x*-chain contains a Kerr nonlinearity, the source beam is set at the left side of the later, while the control beam is located at the top side of the *z*-chain. The control beam can turn ON and OFF the light transmission of an incoming light. We report a theoretical model of a very small all-optical transistor proof-of-conceptmade of optical 'light switching light'concept. We show that the transmission efficiency strongly depends on the control beam and polarization of the incoming light. We investigate the influence of a perfect reflector and reflecting substrate on the transmission of the optical signal when the control beam is turned ON and OFF. These new findings make our unique design a potential candidate for future highly-integrated optical information processing chips.

1. Introduction

The emerging of metallic nanoparticles (MNPs) systems [1-3] paves the way to creating on-chip large-scale integrated all-optical systems. When these optical metallic nanoparticles are arrayed in linear chains, it is possible to transport energy and propagate optical excitations in structures that are much smaller than the operating wavelength of the light [4,5]. This can lead

to designs of novel optical circuits with sizes as small as the operating wavelengths of light. The sub-wavelength circuits are not possible by using conventional integrated optics, since the diffraction limit stands as the main challenge. In the metallic nanoparticles chain, the coherent propagation of the optical signals is conducted by dipolar resonances of a single nanoparticle and mediated by dipole-dipole coupling between neighboring nanoparticles. Along the chain, the transverse width is controlled by the particle size which is in the 100 nm range, this is much smaller than the optical wavelength, $\lambda \approx 350$nm. Also, the strong confinement of the light plays a central role in guiding Surface Plasmon Polaritons (SPPs) in nanosized structures [6,7], as a result, the wavelength of the light propagation is shortened significantly and hence allows the SPPs to travel in a structural geometry with very small transverse dimensions [8,9]. In these MNPs structures the diffraction-limited sizes can be avoided and the realization of optical devices with extremely small mode volumes can be achieved.

The MNPs chains are based on optical devices that emerge as a promising approach for future nanosized circuits and active optical platforms that could be implemented in next generation of optical computers and ultra-high-speed photonic devices and systems. The light propagation along the metal nanoparticles chain was investigated by many researchers [10-12]. Quinten *et al* [13] studied modes propagation in Ag chains under longitudinal excitation. In their study, they have shown that the modes' propagation originates from the dipole moments alignment along the Ag chain axis. The metal nanoparticles chains play a crucial role in overcoming the limitations in the miniaturization of optical integrated circuits. The use of nonlinearity in metal nanoparticles chains may lead to the design and construction of ultra-compact all-optical devices such as an optical transistor that operates in a single chip or chip-to-chip, providing communication and links in a single chip and/or chip-to-chip.

In this research, we consider two monodimensional finite chains of equally spaced metal nanoparticles of radius *a*, separated by a center-to-center distance $d \geq 2a$. These two chains are arranged along the *x* and *z*-axis at the crossing region, where Kerr nonlinearity is introduced. With this proposed structure geometry we construct a proof of concept an all-optical transistor in which the output signal of an incoming light can be turned ON or OFF by controlling the beam with high contrast. Also, we show that the proposed structure allows either the amplification or attenuation of the propagating signal at the rightmost nanoparticle when the control beam is applied. To describe the optical properties such as the transmission spectra and electromagnetic response of the arrayed chains based transistor, a coupled point-dipole approximation is used [14-15].

2. The Proposed Model Structures

The proposed model, illustrated in **Figure 1**, consists of two perpendicular metallic (silver) nanoparticles (MNPs) chains. The first chain contains 7 MNPs placed along the *x*-axis (*x*-chain) where the source beam is set at its left side and the second one contains 4 MNPs placed along the *z*-axis (*z*-chain) where the control beam (gate) is applied at the firstmost. The MNPs of the two chains are identical and spaced at equal distances (R) embedded in a homogeneous medium with permittivity ε^L. We generate the nonlinear optical switching by introducing a Kerr medium at the fourth MNP. These chains are located at a distance (*h*) from a semi-infinite substrate with a permittivity ε_{sub}. For convenience, the schematics of the proposed model and the parameters involved in our calculations are provided in Figure 1. It is worth noting that the leftmost MNP in the *x*-chain is excited by the external field, whereas in the *z*-chain it is the uppermost MNP exposed to the external excitation. The energy transport is maintained across both chains due to the generated surface plasmon around the spherical MNPs and the surface of the metallic substrate. It is worth stressing that the intensity at the rightmost particle in *x*-axis depends strongly on the interaction of the source and control

beams. It is expected that the control beam contributes to the amplification/attenuation of the output signal. In our structure, MNPs are assumed to have equal radii *a*. The external light wave E_0 is chosen to have transversal and longitudinal polarizations and is used to excite both the leftmost nanoparticle in the *x*-chain where the source is set and the uppermost nanoparticle where the control beam (gate) is set, as shown in the Figure 1. Since we are not at this point interested in time development of the optical transmission, we focus entirely on the amplitude of the exciting field. When we shine a neutral metallic nanoparticle in the *x* and *z* chains with an external field, a dipole is created due to the induced charges at the surface of MNPs. At the crossing of the chains and precisely in the forth nanoparticle, there are two main contributions which are the plasmonic field (source and control beams) and Kerr effect. The external light wave E_0 creates a dipole moment *P* on the leftmost and uppermost particles located in the linear medium with a dielectric permittivity ε^L. For the sake of completeness, we introduce a nonlinear medium at the crossing of the chains at the forth MNP. The nonlinear medium has a dielectric permittivity ε^{NL} and a dipole moment P^{NL}.The dipole moments of thelinear and Kerr mediums are expressed as [16-18]

$$P^L = \varepsilon\alpha(\omega)E_0 \qquad (1)$$

$$P^{NL} = \alpha_{Kerr}\varepsilon\chi E^3 \qquad (2)$$

where ω is the angular frequency, $\alpha_{Kerr}$is the nonlinear coefficient of the Kerr medium, χ is the susceptibility of the medium, ε presents the dielectric function of the Kerr medium and $\boldsymbol{E}$ is the sum of the plasmonic fields at $MNP_{(n\text{-}l)}$ generated by the source and the control beam (gate) and $\alpha(\omega)$ is the polarizability of the MNPs given by [3]:

$$\frac{1}{\alpha(\omega)} = \frac{\varepsilon_p(\omega)+2\varepsilon}{\varepsilon_p(\omega)-\varepsilon}\frac{1}{a^3} - \frac{k^2}{r} - \frac{2i}{3}k^3 \qquad (3)$$

where $\alpha(\omega)$ stands for the polarizibility of the MNP, $\varepsilon_p(\omega)$ is the permittivity of the MNPs, $k = (\omega/c)\,\varepsilon^{(1/2)}$ is the wave number in the background medium of MNPs, c is the speed of light and r is the position of the detector.

The ***E*** field is expressed as follows:

$$E = E^{source}_{plasmon,\ (n-1)} + E^{gate}_{plasmon,\ (n-1)} \quad (4)$$

The term k^2/r describes the depolarization shift while $2ik^3/3$ accounts for the radiative damping. It is worth noting that the polarizability is strongly dependent on the frequency ω and can be negative in a certain frequency range. In present contribution, the second and third corrective terms in polarizability expression associated with weak effects are involved in our calculations. In this case, it is possible to see that the resonance of the localized surface Plasmon satisfies the condition *Re* ($\varepsilon(\omega)$) = -2 ε [19]. We use the Green function to calculate the emitted electric field ***E*** generated by the dipole moment ***P***, where ***E*** and ***P***are given as:

$$P = P^{L} + P^{NL} \qquad (5)$$

The ***E*** field is related to the dipole moment as:

$$E = \frac{1}{\varepsilon}k^2 G(r,r')P \qquad (6)$$

where $G(r, r')$ is the Green function, r' and r represent the position of the source and the detector respectively. When the spherically oriented MNP placed in a medium are irradiated by an external field, there are various charge configurations that enable contribution to the scattered field. We particularly assume that the dipole moment is the major contributor where we replace each MNP by a simple point dipole. Among the interactions taking place in the chains, the dipole-dipole interaction is considered according to the following conditions $a<<\lambda$ and ($R >> 3a$) where λ is the operating wavelength. With this interaction, we focus only on the fundamental mode since all excited modes are neglected [20]. The involved dipole moment is calculated using the corresponding Green's function technique. It is well known that the Green's function, for an arbitrary scattering charge system and nonmagnetic medium, can be obtained by solving (2) the wave vector equation [21]:

$$\nabla \times \nabla \times G(r,r') - k^2 \varepsilon \nabla \times G(r,r') = I\delta(r-r') \qquad (7)$$

As it has been shown elsewhere that for a homogenous medium the solution of Eq.7 is [22]:

$$G^H(r,r') = \frac{\exp(ikR)}{R}\left[\left(1+\frac{ikR-1}{k^2R^2}\right)I + \frac{3-3ikR-k^2R^2}{k^2R^2}\frac{RR}{R^2}\right] \qquad (8)$$

where $R = |r - r'|$ indicates the distance from the source r' to the detection point r, $\boldsymbol{I}$ is the unit matrix and the quantity RR is the auto-product of two matrices.

The dipole moment of a MNP here is induced by the scattered field from the other metallic spheres in the vicinity and the substrate. With this background, the dipole moment of each MNP can be obtained by solving the following equations [23]:

$$P_1 = \alpha_1 E_0(r_1) + \frac{k^2}{\varepsilon}\alpha_1 G^H(r,r')P_1 + \frac{k^2}{\varepsilon}\sum_{j\neq 1}^{N}\alpha_1\left(G^H(r_1,r_j) + G^S(r_1,r_j)\right)P_j \qquad (9)$$

where r_i and α_i are the position of the center and the polarizability of the particle number *i*, and $G^S(r, r')$ is a Green' tensor introduced in order to take into account the reflected wave from the substrate (MNPs-substrate interaction). $G^H(r, r')$ which is shown in eq. (8) describes the interaction between MNPs.

The dipole moments induced in the chain of metal particles located close to the dielectric-metal interface can be determined by considering the following equations;

$$\sum_{\mathbf{m}}\left[\frac{1}{\alpha}\delta_{\mathbf{n,m}} + \left(\mathbf{G}^{\mathbf{H}}_{\mathbf{n,m}} + \mathbf{G}^{\mathbf{S}}_{\mathbf{n,m}}\right)\right]\mathbf{p}_{\mathbf{m}} = \mathbf{E}_{\mathbf{m}} \qquad (10)$$

Rewriting equation (9a) as an eigen problem expressed as:

$$\hat{\mathbf{M}}\mathbf{p} = \mathbf{E} \qquad (11)$$

Where $\delta_{\mathbf{n,m}}$ is the Kronecker delta, $\hat{\mathbf{M}}$ is a 3N-b-3N matrix and the dipole vector $\mathbf{p}$ is 3N-components vector and the applied electric field $\mathbf{E}$ is 3N-components vector.

Here, we introduce the interaction of the control beam with the source. The effects of the Kerr medium on the output filed $\boldsymbol{E}_{out}$ are also taken into consideration through the calculation of the dipole moment generated at the 4-MNP in the *x*-chain. The dipole moment generated (at the crossing medium fourth MNP) is the sum of two contributions, which are; the source field and the control beam. The expression of the output field $\boldsymbol{E}_{out}$ is given by the following equation (12):

$$\mathbf{E}_{out} = \frac{1}{\varepsilon}\sum_{m=1}^{N_s}\left[\frac{1}{\alpha}\delta_{nm}\mathbf{I} - \mathbf{k}^2\left(\mathbf{G}^H(\mathbf{r}_n,\mathbf{r}_m) + \mathbf{G}^S(\mathbf{r}_n,\mathbf{r}_m)\right)\right]\mathbf{P}_m + \frac{1}{\varepsilon}\sum_{p=1}^{N_c}\left[\frac{1}{\alpha}\delta_{np}\mathbf{I} - \mathbf{k}^2\mathbf{G}^H(\mathbf{r}_n,\mathbf{r}_p)\right]\mathbf{P}_p - \frac{\mathbf{k}^2}{\varepsilon}\sum_{n=1}^{N_s}\sum_{c=1}^{N_c}\mathbf{G}^C(\mathbf{r}_n,\mathbf{r}_c)\mathbf{P}_c \quad (12)$$

where ***I*** is the unit matrix, N_S and N_c are the number of MNPs in the *x*-chain (source) and *z*-chain (control) respectively and r_n is the position of the n^{th} MNP. The first term, '*m*'-term, describes the contribution of the source, the second term, '*p*'-term, represents the contribution of the control beam, and the coupling of the source and control beam is described by the third term, '*c*'-term, in the above equation.

3. Results and Discussions

In this section, we consider two linear cross-chains along the *x*- and *z*-axes respectively. The *x*-chain is formed of 7 spherical MNPs most of which are embedded in a linear medium with permittivity ε^L except for the fourth one which is assumed to be placed in a Kerr medium with nonlinear permittivity ε^{NL}. The *z*-chain contains three MNPs identical to those in *x*-chain. The source beam is a point-dipole set at the left side of the *x*-chain exciting the leftmost nanosphere. The control beam is set on the top of the *z*-chain and similarly excites the firstmost MNP. The field at the 4^{th} nanosphere is the sum of the fields due to all other dipoles in the *x*-and *z*-chains, the induced moment is the polarizability times the total field. To describe the optical response of the proposed device, we calculate the transmission of an optical excitation (source beam) through the chain when the control beam is turned ON and OFF. In other words, our intention is to fine-tune the control beam to increase the transmission efficiency at its maximum value when the control beam is ON and to reduce the transmission efficiency to zero when the control beam is OFF. This demonstrates the source-control beam coupling.

In our calculations, we consider the *x*-chain parallel to a perfect reflector and the following parameters; the distance from the *x*-chain axis to the reflector (*h*) =50 nm, ((*h* ≥ 3*a*/2): condition to maintain the dipole approximation), the MNP spacing is (*d*) = 75 nm and the radius (*a*) = 25 nm (as shown in **Figure 1**).

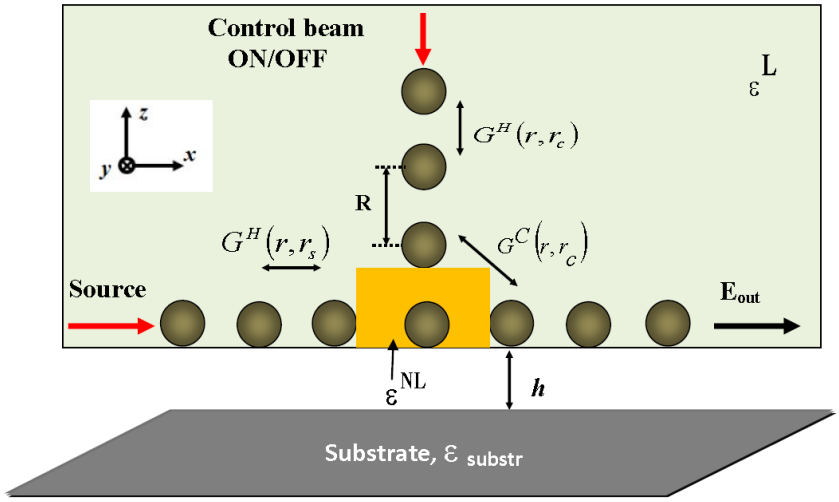

Figure 1. Schematics of the proposed transistor that consists of two perpendicular chains of identical MNPs: an *x*-chain contains 7 equidistant spherical MNPs embedded in a linear medium with a permittivity ε^L expect the fourth MNP is placed in a Kerr medium with a nonlinear permittivity ε^{NL}. The *z*-chain contains 4 identical MNPs, in both chains the MNPs are equidistant and spherical with a radius *a* = 25 nm. The *x*-chain is at a distance of *h* = 50 nm from the substrate. The source is set at the left side of the *x*-chain where the leftmost MNP is considered to be excited, whereas the control beam is located at the top of the *z*-chain, the uppermost MNP is considered to be excited.

3.1Effect of the Polarizations

In our calculation, the contribution of the substrate is introduced by adopting the technique of image [24]. In this approach, the substrate is substituted by an image of MNPs of the same size and placed at equal distance but in the opposite side of the surface. As a result, the substrate can be replaced by the mirror image of the induced dipole. In our calculations, in order to take into account the reflected waves from the substrate, we have introduced the Green's tensor $G^S(r, r')$ describing the chain-substrate interaction, which has the similar expression $G^H(r, r')$.

Firstly, while the source is longitudinally polarized and the control beam is transversally polarized, we calculate the transmission efficiency T for two states of the control beam: ON and OFF; the obtained results are reported in **Figure 2**.

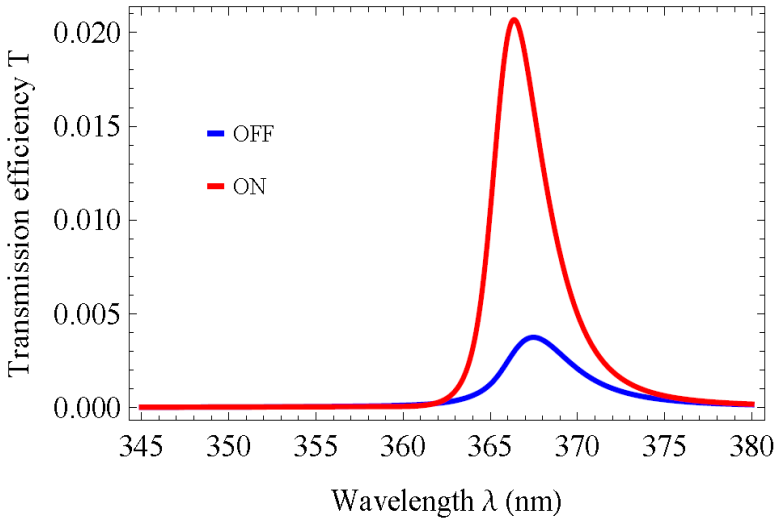

Figure 2. Transmission efficiency T as a function of the excitation wavelength λ for *x*- and *z*-chains of 7 and 4 spherical identical MNPs, respectively. The radius *a* is 25 nm, interparticle spacing *d* is 50 nm, and a separation *x*-chain-substrate of 50 nm. The source is longitudinally polarized (along x-axis) and the control beam is transversally polarized (along *x*-axis).

This Figure shows two peaks for both states of the control beam (ON and OFF). The left peak (the curve in red color) is more intense than the right one when the control is ON. However, in the case when the control beam is turned OFF the right peak (the curve in blue color) increases and a shift to longer wavelengths (redshift) is observed. The small peaks originate mainly from the reflecting interface. The reflected field together with the field of the nanoparticles interfere destructively which in return results in a weak coupling between those MNPs and a weak transmission of the optical excitation through the chain is observed. In the case when the control beam is ON, the intense peak is as high as 20 times the one when the control beam is OFF. Comparing the transmission spectra when the control beam is ON and OFF, as shown in Figure 2, points the effect of the control beam on the output field of the proposed device. Inspecting Figure2, in the absence of the control beam and for a parallel polarization, the dipole moments of MNPs interact with the induced image dipoles in the perfectly reflecting substrate and form quadrupoles which reduce the interaction between MNPs in the *x*-chain. As a result, a weak transmission is observed.

For *z*-polarized excitations of both, the source is transversally polarized and the control beam is longitudinal polarized, the transmission through the MNPs chain is performed and shown in **Figure 3**. In the presence of the control beam (the curve in red color) the peak is much more intense than that obtained when the control beam is turned OFF. Comparing the transmission in both cases, a strong dependence of the output response of the transistor on the control beam is demonstrated. The increase in the transmission spectra, shown in Figure3, results mainly from the coupling between MNPs in the source and the control beams. This coupling prevents the MNPs in source chain to form effective quadrupoles together with their induced image dipoles. The dipole-dipole interaction gives rise to a stronger coupling between MNPs along the *x*- and *z*-chains. However, the coupling between neighboring MNPs reduces the restoring

forces, which in turn affects the coupling between the MNPs in the control beam and those in the source beam chain. The small peaks, in presence and absence of the control beam, originate from the fact that the dipole moment of the MNP is orthogonal to the substrate couples to the induced image dipole, in return the restoring forces are reduced and as a result, the transmission decreases.

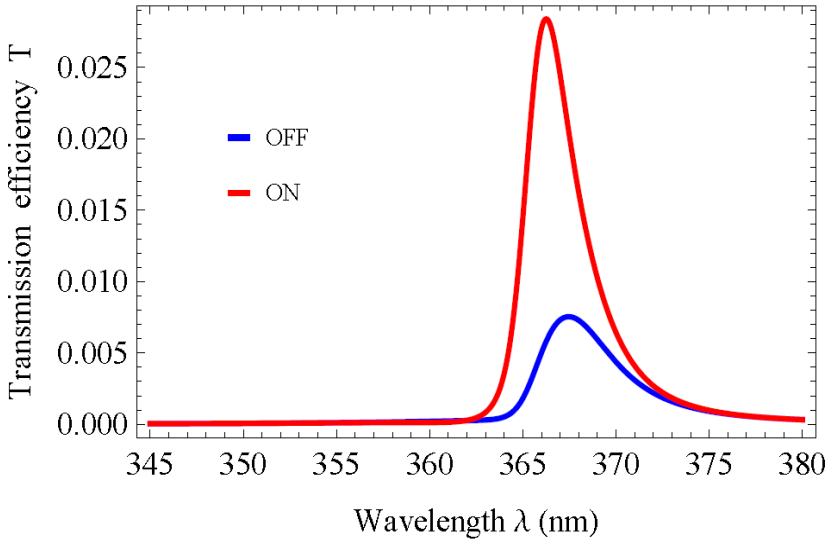

Figure 3. Transmission efficiency T as a function of the excitation wavelength λ for a transversal polarization for the source beam and a longitudinal excitation for the control beam two cases are considered: The curve in blue color shows the case when the control beam is OFF, the curve in red color shows the case when the control beam is ON. The number of MNPs in both chains is kept unchanged.

Next, the polarization of the source is kept *z*-polarized (transversal) while the control beam is *x*-polarized (transversal). The dipole moment of the spherical MNPs along the *x*-chain is orthogonal to the substrate that interacts resonantly with the induced dipole moment. Transmission efficiency T as a function of the wavelength λ for this case is illustrated in

Figure 4. Because of this strong interaction the restoring force in the control beam chain is increased by neighboring MNPs, so the net coupling from the control beam to the source beam (*x*-chain) is much stronger than the previous case. The MNPs dipole moments in the control chain are not cancelled out with the induced images, therefore they interact with the source beam and contribute to the optical signal propagation along the *x*-chain. In return, as can be seen in Figure 4, when the control beam is ON an increase in the transmission efficiency is obtained when compared to previous obtained results shown in Figure 2 and Figure 3. As it can be observed from Figure 4, the effect of the control beam in the transmission efficiency is evident. This Figure demonstrates a strong dependence of the chains transmission on the control beam. In particular, this property opens up the opportunity to design footprint devices such as optical transistors.

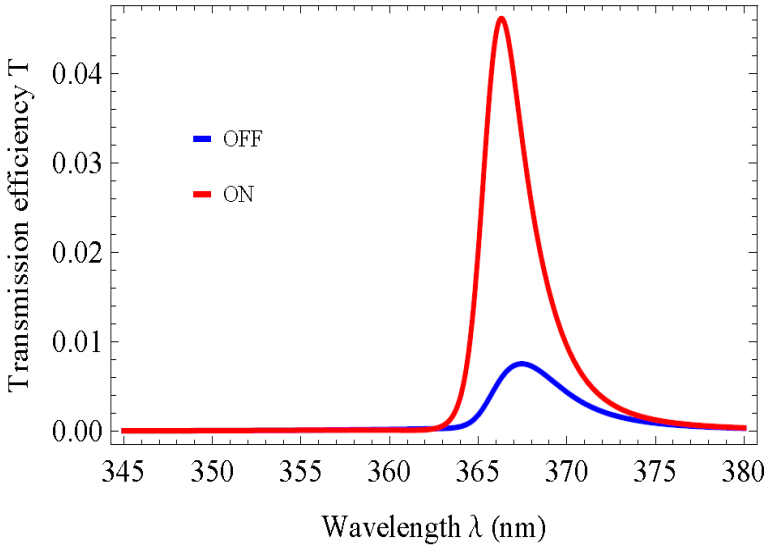

Figure 4. Transmission efficiency T as a function of the excitation wavelength λ for the proposed transistor that consists of a source (*x*-chain)of 7 identical MNPs a control beam (*z*-chain) contains 4 identical MNPs, in both chains the silver particles are spherical with a radius of 25 nm and center-to-center spacing of 50 nm, for two situations of the control beam: The curve in blue color shows the case when the control beam is OFF, the curve in red color

shows the case when the control beam is ON. The source is polarized along *z*-axis (transversal polarization) and the control beam is x-polarized (transversally polarized: excitation along *x*-axis).

To explore how the control beam affects the output of the *x*-chain, we reverse the polarization of the source and the control beams. In this case the source is longitudinally polarized (excitation along the x-axis), while the control beam is *z*-polarized (longitudinal polarization). In **Figure 5**, we have illustrated the transmission efficiency T as a function of the wavelength λ when the control beam is ON (shown by the curve in red color) and OFF (shown by the curve in blue color). It should be noted that the transmission of the *x*-chain contains one predominant peak, corresponding to the control beam effect on the propagating excitation. The other small peaks come from the fact that the dipole moment of the MNP of the *x*-chain longitudinally polarized is cancelled out by the induced image dipoles. As it can be seen from Figure5, there is a significant decrease of the transmission efficiency when the control beam is *z*-polarized. The decrease in the transmission efficiency in the presence of the control beam compared to the case where both the source and the control beam are *x*-polarized (the source is longitudinally polarized and the control beam is transversally polarized) is due to the weak coupling of the control beam to the light source and the weak interaction of the neighboring MNPs along the *x*-chain.

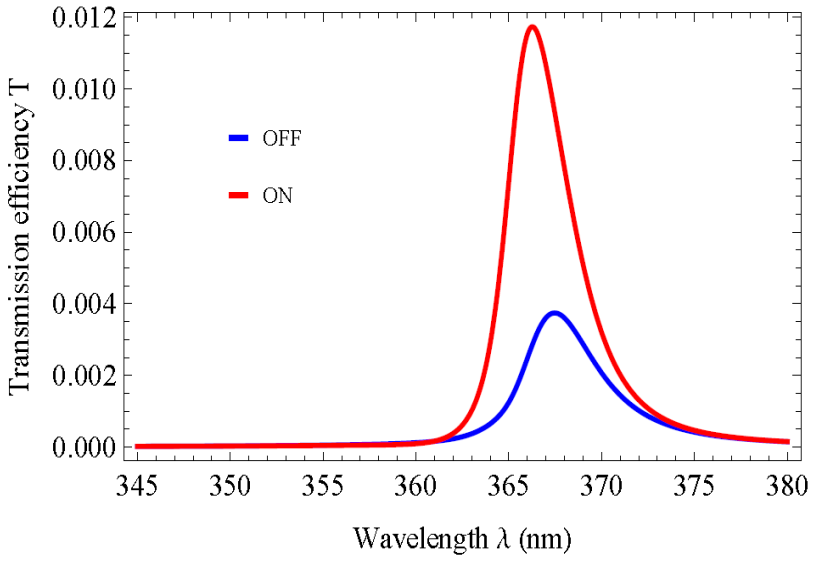

Figure 5. Transmission efficiency T as a function of the excitation wavelength λ for an *x*-array of 7 MNPs with a radius of 25 nm, interparticle spacing of 50 nm, and a separation *x*-chain-substrate of 50 nm and an *z*-array of 4 MNPs, which are identical to those in *x*-chain. The excitation of the source is on the leftmost MNP with polarization along the chain *x*-axis (longitudinal). The excitation of the control beam is on uppermost MNP with polarization along the *z*-axis (longitudinal). The curve in blue color shows the case when the control beam is OFF, the curve in red color shows the case when the control beam is ON.

3.2 Energy Transfer and the Coupling of the Chains to the gold Substrate

The Surface Plasmons (SPs) are generated at the metal-dielectric interface, these confined elementary excitations depend strongly on the structural parameters and geometry of the metallic surface [25] and on the dielectric function of the proximate medium [26]. The surface plasmons can be delocalized and propagated when they are deposited on a metallic surface or a film [27]. In this context, when a gold substrate is placed in the vicinity of the MNPs chain, some part of the energy is not reflected and excites the surface modes creating SPPs. The dipole moment in the *x*-chain creates parallel and effective dipole moments on the substrate; we assume that these dipole moments have the same amplitude. The substrate is considered as an effective chain of identical MNPs and is parallel to the principal chain and located at $z = -h$, as it is illustrated in **Figure 6**.

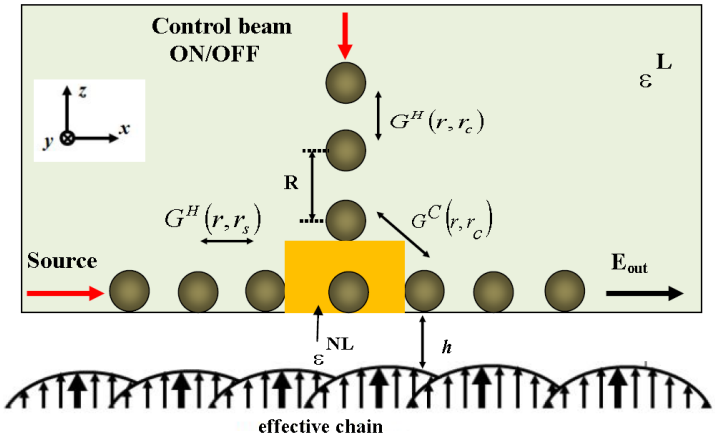

Figure 6. Schematic of the proposed transistor composed of 7 MNPs arrayed in the *x*-chain incorporating a Kerr nonlinearity and 4 identical MNPs in *z*-chain located in close proximity to a metal (gold) substrate. In our model the substrate is considered as an effective chain of identical and equidistant MNPs with permanent dipole moments. The small difference between the values of plasma frequency of both metals silver (MNPs) and gold (substrate) lead to a quasi-identical interactions silver-silver and silver-gold.

To observe the influence of the chain on the performance of the transistor for different states and polarization of the source and the control beams on the transmission efficiency of the optical signal, we proceed the same way with the case of the perfect reflector. The control beam is polarized along the z-axis (longitudinal polarization) while the source beam is transversally polarized (polarized along the *z*-axis) and obtained results of the transmission efficiency as a function of the wavelength when the control beam is ON and OFF are illustrated with red curve and blue curve, respectively in **Figure 7**.

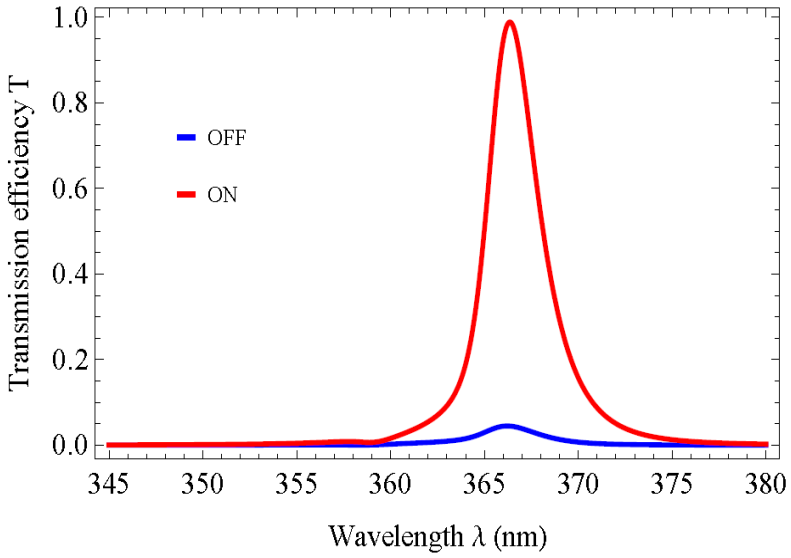

Figure 7. Transmission efficiency T, as a function of wavelength λ for the proposed device where the *x*-chain is 50 nm above the gold substrate. The source is excited along *z*-axis and the control beam is transversally polarized (excited along the x-axis). The transmission is performed for two states of the control beam: The curve in blue color shows the case when the control beam is OFF, the curve in red color shows the case when the control beam is ON.

It is clear from this figure that when the control beam is turned ON, the transmission is about 1 and exhibits a peak centered at λ = 367 nm, however when the control is turned OFF, it drops to around 0.05. We notice a substantial increase in the transmission efficiency compared to the perfect reflector substrate case. This is originated from the coupling of the SPPs to the MNPs. It should be stated that the SPPs are confined modes at the interface, the coupling to the MNPs allows the light to scatter into the far-field and therefore increases the output field at the last MNP of the *x*-chain. It should be noted that the obtained results for the perfect reflector case are illustrated in figures 2, 3, 4 and 5, and there is no excitation of surface polaritons at the surface of the reflector (substrate), however, when we have used gold as a substrate (illustrated in Figure 6 and the rest of figures (6-11)), we are able to excite the

surface polariton which in turn couple to the surface plasmons of MNPs in *x*-chain then propagate and increase the output field, E_{out}.

Next we investigate the inverse of the polarization on the proposed device. In this case, the source is excited along the *x*-axis (longitudinal) while the control beam is excited along the z-axis (longitudinally polarized). The obtained results are depicted in **Figure 8**. As can be seen from this figure, when the control beam is ON, the transmission efficiency is significantly higher than when the control beam is OFF, (the curve in blue color). In fact when the control beam is OFF, the transmission is almost flat (zero). Nevertheless, the transmission efficiency, when the control beam is ON, is much smaller than previous case obtained in Figure 6, and it is much higher than obtained results illustrated in figures (2, 3, 4, and 5). Furthermore, there is a major improvement on the transmission efficiency, (it is almost zero when the control beam is OFF, shown by the curve in blue color) when compared to previous obtained results in figures (2, 3, 4, 5).

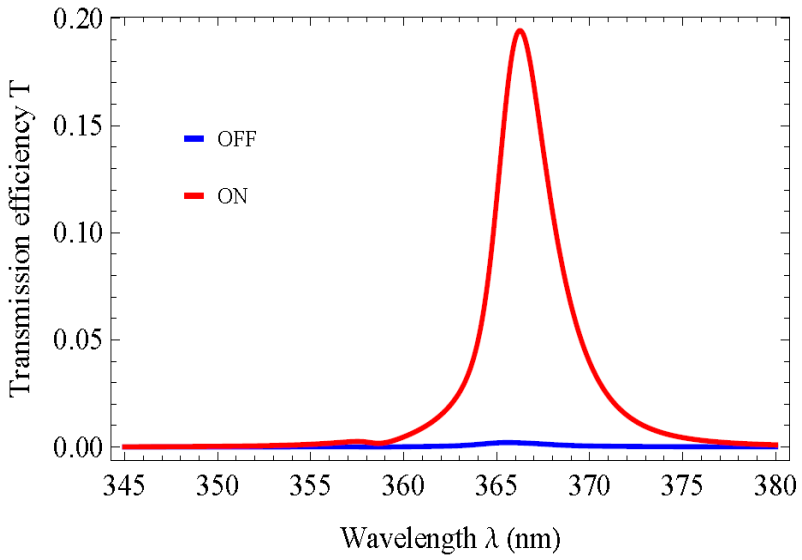

Figure 8. Transmission efficiency T, as a function of wavelength λ for the proposed device where the *x*-chain is 50 nm above the gold substrate. The source is excited along *x*-axis while the control beam is longitudinally polarized (excited along the z-axis). The transmission is performed for two states of the control beam: The curve in blue color shows the case when the control beam is OFF, the curve in red color shows the case when the control beam is ON.

Next, the source is longitudinally polarized and the control beam is transversally polarized (excited along the x-axis), and the transmission efficiency is calculated as a function of the wavelength and reported in **Figure 9**. In this case, we notice an increase in the transmission compared to the perfect reflector substrate case. Also, the difference between perfect and non perfect substrates, like gold, is clear when comparing the small peak (the curve in blue color). It can be observed that the amplitude increases and slightly red shifts. As expected, we observe an increase of the transmission in presence of the control gate as compared to the case of the perfect reflector. This can be explained by the fact that an amount of the light is not reflected by the substrate and excites the SPP modes, in return, the later couple to the MNPs along the *x*-chain and contribute to the optical signal.

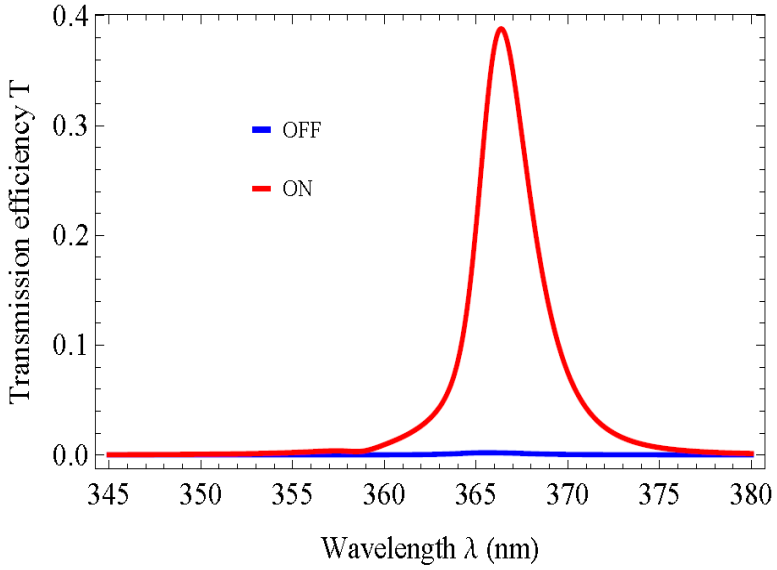

Figure 9. Transmission efficiency T as a function of the excitation wavelength λ for an *x*-array of 7 MNPs with a radius of 25 nm, interparticle spacing of 50 nm above the gold substrate, and a separation *x*-chain-substrate of 50 nm and an *z*-array of 4 MNPs, which are identical to those in *x*-chain. The excitation of the source is on the leftmost MNP with polarization along the chain *x*-axis (longitudinal). The excitation of the control beam is on uppermost MNP with a polarization along the *x*-axis (transversal). The curve in blue color shows the case when the control beam is OFF, the curve in red color shows the case when the control beam is ON.

To gain more insight into the dipole orientations, we excite both the source and the control beams along *z*-direction, the source is transversally polarized while the control beam is longitudinally polarized. The calculated transmission efficiency as a function of the wavelength is shown in **Figure 10**. If we compare the transmission efficiency shown in Figure10 to those results obtained and shown in Figure 2 in presence of a perfectly reflecting substrate we notice that the peaks of the transmission efficiency increase in both cases when the control beam is ON and OFF.

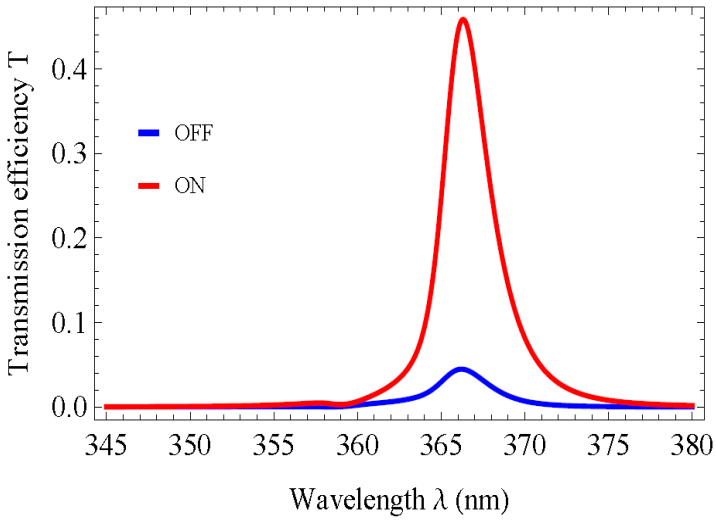

Figure 10. Transmission efficiency T as a function of the excitation wavelength λ for an x-array of 7 MNPs with a radius of 25 nm, interparticle spacing of 50 nm above the gold substrate, and a separation *x*-chain-substrate of 50 nm and an *z*-array of 4 MNPs, which are identical to those in *x*-chain. The excitation of the source is on the leftmost MNP with a polarization along the chain *z*-axis (Transversal), the excitation of the control beam is on uppermost MNP with a longitudinal polarization. The curve in blue color shows the case when the control beam is OFF, the curve in red color shows the case when the control beam is ON.

This increase is due to the fact that the dipoles which are perpendicular to the gold substrate resonantly couple to the induced image dipoles, thus the restoring forces increase and the interaction between neighboring MNPs becomes stronger compared to longitudinal polarizations. Since the SPPs are excited at the surface, they will mediate the coupling between dipoles and increase the transmission efficiency. Also, the oscillating dipoles interact with both transverse electric and magnetic surface waves. This will enhance the transmission of the proposed device. Figure10 shows the transmission efficiency when both the source and the control beams are z- polarized. Compared with the reported results shown in Figure9 when the source is transversally polarized and control beam is longitudinally polarized, the transmission efficiency decreases since the dipole moments in the source chain will form with their induced dipole images quadripoles, therefore the restoring forces are reduced and the coupling between neighboring MNPs along the source are in return decreased.

3.3 Amplification and Attenuation

In this section, we investigate how the control beam will amplify and/or attenuate the output signal when two states (situations/cases) are considered. Here we introduce the following relationship:

$$I'_{control} = I^{0}_{control} \times \beta \qquad (13)$$

where $I'_{control}$ and $I^{0}_{control}$ represent the control beam optical signals with (when the control beam is multiplied by the factor β) and without (when the control beam is not multiplied by the factor β) action respectively, and where β stands for the amplification factor. The amplification case is considered where the control signal is multiplied by a factor of β = 1.5, β = 2 and β = 2.5. The obtained results are shown in figures 11 (a, b, c). The amplification factor β is used to increase or attenuate the output signal by action of the control beam.

Figure 11 shows the transmission efficiency as a function of the wavelength when the source is *z*-polarized and the control beams is longitudinally polarized. When the amplification factor β is gradually increased from 1.5 to 2.0 and then to 2.5, as expected, the output signal is increased as the amplification factor β is increased. The transmission efficiency exhibits a dominant peak centered at λ = 366 nm, which corresponds to the ON state, however this peak drops to 0.01 when the control signal is turned OFF, as illustrated in Figure 11 (a, b, and c). If we compare the transmission obtained in Figure 2 (section effect of the polarization) to that shown in Figure 11 (a, b, c), it is obvious that the maximum transmission efficiency increases significantly from 0.02 to 0.8 when β = 2.5. In other words, a substantial increase of the transmission efficiency is obtained when the amplification factor β is equal to 2.5. When the

obtained results of the transmission efficiency in Figure 10(c) are compared with those in Figure 4, we can clearly see almost zero transmission efficiency when control beam is OFF, as shown in blue color in Figure 11 (c). In other words, the overall performance of the proposed configuration depends strongly on the control beam state as it has been improved considerably when the amplification factor β = 2.5.

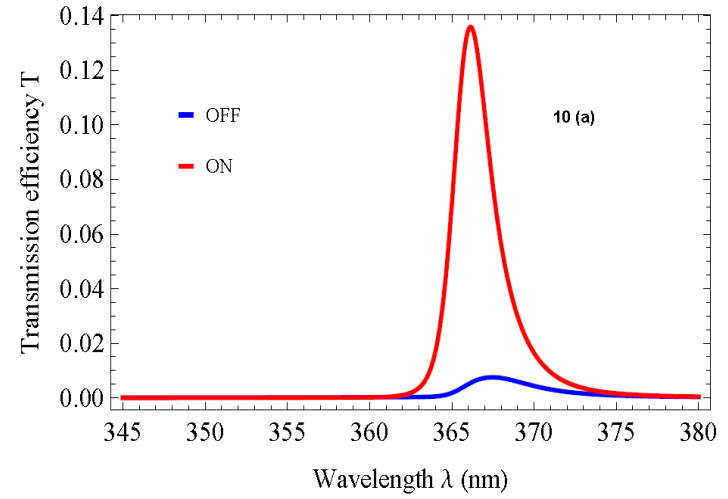

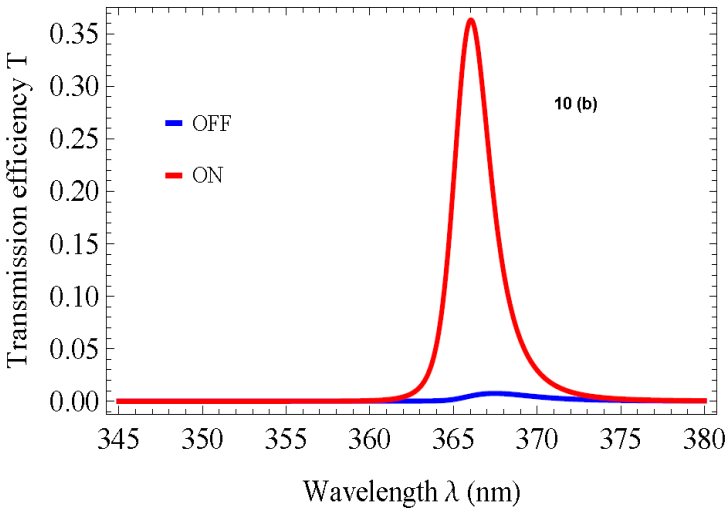

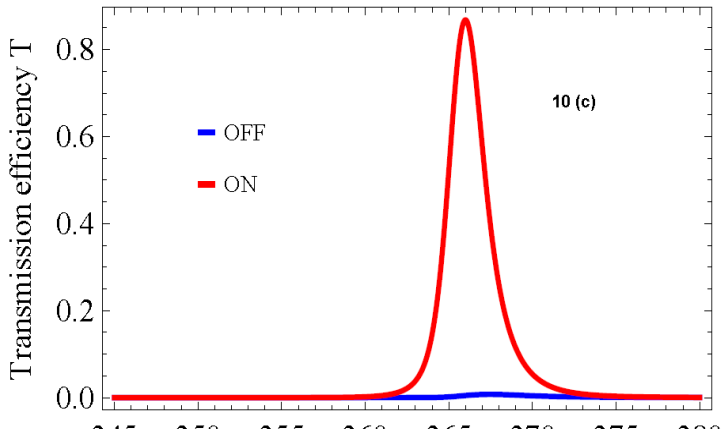

Figure 11. Amplified transmission efficiency T of the 7 MNPs *x*-array with a radius of 25 nm, interparticle spacing of 50 nm, and a separation *x*-chain-substrate of 50 nm and in *z*-array of 4 MNPs. The excitation of the source is on the leftmost MNP with polarization along the chain *x*-axis (longitudinal). The excitation of the control beam is on uppermost MNP with transversal polarization (x-axis) for various values of the amplification factor: a) β = 1.5, b) β = 2 and c) β = 2.5. The curve in blue color shows the case when the control beam is OFF, the curve in red color shows the case when the control beam is ON.

Next we investigate the attenuation as a function of the wavelength. In order to analyze the attenuation, we keep the same polarization of the source and control beam, and we reduce the attenuation factor β to 0.5. The transmission efficiency for β = 0.5 is illustrated in **Figure 12**. As it can be seen from this figure the transmission efficiency drops significantly to 0.015. The control beam changes the output signal from amplification to attenuation and this can be seen clearly in both Figure 11(a, b and c) and Figure 12. We have fully analyzed the effect of the control beam (gate) on the source and therefore on the output of the proposed model for various values, and for various polarizations and so we have finally obtained the optimized value for β= 2.5, which shows maximum transmission efficiency, as illustrated in Figure 11 (c). In other words, the best obtained results of the transmission efficiency of the proposed all-optical transistor are when amplification factor is set β = 2.5, as illustrated in Figure 11 (c).

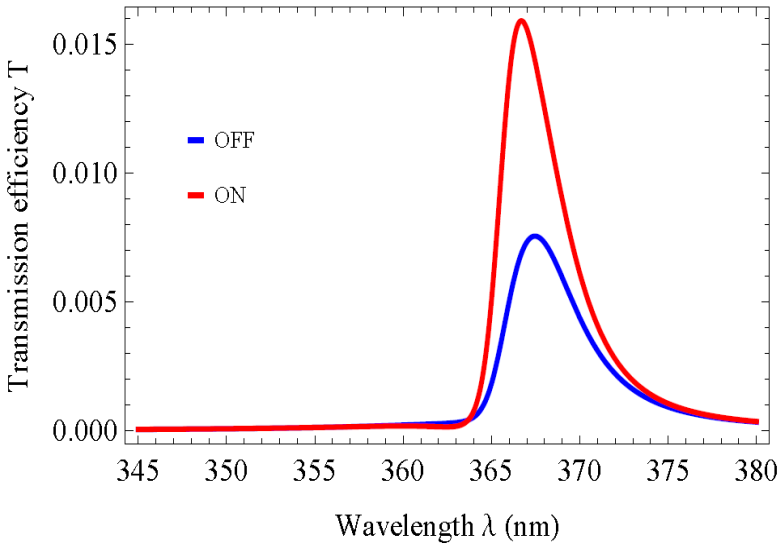

Figure 12. Transmission efficiency T as a function of the excitation wavelength λ for the considered structure. The excitation of the source is along the x-axis and that of the control beam is along z-axis, the control beam after action is $I_{control}^{'} = I_{control}^{0} \times 0.5$. The curve in blue color shows the case when the control beam is OFF, the curve in red color shows the case when the control beam is ON.

4. Conclusion

In summary, we have proposed and demonstrated a proof-of-concept of all-optical transistor by considering two perpendicular silver nanoparticles chains, where the fourth metallic nanoparticle in the longitudinal chain, is placed in a Kerr medium. We have demonstrated that by turning the control beam ON and OFF, light transmission efficiency with a high extinction ratio can be obtained. We have reported that the polarization of both the source and the control beams affect, strongly, the interaction of the neighboring dipoles; when the source beam is transversally excited, the transmission increases and reaches 0.8 while this value drops to less than 0.2 when it is *x*-polarized. Compared to a perfect reflector, we have found that the presence of a real substrate, like gold, contributes enormously to the energy transport

along the *x*-chain giving rise to an increase in transmission. The polarization effects of the control beam on the attenuation and the amplification of the output signal of the proposed optical transistor have been demonstrated. To the best of our knowledge, we have demonstrated a proof-of-concept of a novel all-optical transistor based on optical 'light switching light'conceptwhich is unique and has great potential for the future to contribute to all-optical integrated ultra-high-speed devices and systems.

Acknowledgements: Fathi AbdelMalek proposed the model structures configuration. Fathi AbdelMalek and Walid Aroua performed the effect of the polarizations with assistance from Shyqyri Haxha. Shyqyri Haxha performed Energy transfer and the coupling of the Chains to the substrate, and organised, coordinated and led the writing of the proposed work with assistance from Fathi AbdelMalek. Ian Flint has contributed with inputs from the industry on the Energy transfer and the coupling of the Chains to the substrate.

Received: ((will be filled in by the editorial staff))
Revised: ((will be filled in by the editorial staff))
Published online: ((will be filled in by the editorial staff))

Keywords: Integrated optics, Optical transistor, Kerr nonlinearity, Surface plasmon polaritons.

References

[1] Z. Li, S. Butun, and K. Aydin, Touching gold nanoparticle chain based plasmonic antenna arrays and optical metamaterials, *ACS Photon*. **1**, 228-234, (2014).

[2] L. O. Herrmann, V. K. Valev, C. Tserkezis, J. S. Barnard, S. Kasera, O. A. Scherman, J. Aizpurua, and J. J.Baumberg, Threading plasmonic nanoparticle strings with light, *Nature (London) Commun.***5**, 4568 (2014).

[3] P. J. Compaijen, V. A. Malyshev, and J. Knoester, Surface-mediated light transmission in metal nanoparticle chains, *Phys. Rev. B***87**, 205437 (2013).

[4] Ch. Lee, M. Tame, J. Lim, and J. Lee, Quantum plasmonics with a metal nanoparticle array, *Physical Review A*. **85**, 063823 (2012).

[5] D. K. Gramotnev and S. I. Bozhevolnyi, Plasmonics beyond the diffraction limit, Nature Photonics **4**, 83–91 (2010).

[6] C.L. Nehl, H. Liao, J. Hafner, Optical properties of star-shaped gold nanoparticles, *Nano Lett.*, **6**, 683 (2006).

[7] J.J Mock, D. R Smith,S. Schultz, Local refractive index dependence of plasmon resonance spectra from individual nanoparticles, *Nano Lett.*,**3**, 485 (2003).

[8] Th. Roger , S. Vezzoli, E. Bolduc , J. Valente, Julius J.F. Heitz , J. Jeffers, C. Soci, J. Leach , Ch. Couteau, N. I. Zheludev, D. Faccio, Coherent perfect absorption in deeply subwavelength films in the single-photon regime, Nature Commun. **6**, 7031(2015).

[9] J. A. Dionne, L. A. Sweatlock, H. A. Atwater, and A. Polman, Plasmon waveguides with subwavelength-scale localization, *Phys. Rev. B***73**, 035407 (2006).

[10] J. A. Dionne, H. J. Lezec, and H. A. Atwater, Highly confined photon transport in subwavelength metallic slot waveguides, *Nano Lett.*,**6**, 1928 (2006).

[11] S. Lal, S. Link and N. J. Halas, Nano-optics from sensing to waveguiding, Nature Photonics **1**, 641 - 648 (2007).

[12] M. Quinten, A. Leitner, J. R. Krenn, and F. R. Aussenegg, Electromagnetic energy transport via linear chains of silver nanoparticles, *Opt. Lett.*,**23**, 1331 (1998).

[13] S. Linic, P. Christopher, D.B. Ingram, Plasmonic-metal nanostructures for efficient conversion of solar to chemical energy. Nature Materials, **10**, 911 (2011).

[14] M. L. Brongersma, J. W. Hartman, and H. A. Atwater, Nanoparticle chain arrays below the diffraction limit,*Phys. Rev. B*, **62**, R16356 (2000).

[15] S. Y. Park and D. Stroud, Surface-plasmon dispersion relations in chains of metallic nanoparticles: an exact quasistatic calculation, *Phys. Rev. B***69**, 125418 (2004).

[16] D. S. Citrin, Plasmon-polariton transport in metal-nanoparticle chains embedded in a gain medium, *Opt. Lett*. **31**, 98 (2006).

[17] J. V. Hernandez, L. D. Noordam, and F. Robicheaux, Asymmetric response in a line of optically driven metallic nanospheres, *J. Phys.Chem. B***109**, 15808 (2005).

[18] A. Taflove, S.C. Hagness, Computational Electrodynamics: The Finite-Difference Time-Domain Method, *second ed., Artech House, Boston*, (2000)

[19] S. A. Maier, Plasmonics: Fundamentals and Applications, (*Springer, New York*), (2007).

[20] L.J. Sherry,S.H. Chang, G.C.Schatz,R.P. Van Duyne, B.J. Wiley,Y.N. Xia,. Plasmon resonances of a gold nanostar, *Nano Lett*. **4**, 2034 (2001).

[21] Ph. Gay-Balmaz, O. J.F. Martin, Validity domain and limitation of non-retarded Green's tensor for electromagnetic scattering at surfaces, *Computer Physics Communications***144**, 111 (2002).

[22] L. Novotny and B. Hecht, Principles of Nano-Optics, *Cambridge University Press*, Cambridge, England (2006).

[23] A.B. Evlyukhin and S.I. Bozhevolnyi, Near-field probing of photonic crystal directional couplers, *Laser Phys. Lett.*,**3**, 296 (2006).

[24] J. D. Jackson, Classical electrodynamics, *third edition, New York: John Wiley & Sons ISBN 0-471-30932* (1998).

[25] A. B. Evlyukhin and S. I. Bozhevolnyi, Point-dipole approximation for surface plasmon polariton scattering: Implications and limitations, *Phys. Rev. B***71**, 134304 (2005).

[26] J. J. Mock, R. T. Hill, A. Degiron, S. Zauscher, A. Chilkoti, D. R. Smith, Distance-dependent plasmon resonant coupling between a gold nanoparticle and gold film, *Nano Lett.*,**8**, 2245 (2008).

[27] T. Chen, M. Pourmand, A. Feizpour, B. Cushman, and B. M. Reinhard, Au Nanoparticle Chains through Simultaneous Control of Size and Gap Separation, *J. Phys. Chem. Lett*. **4**, 2147 (2013).

Graphical Abstract

We have proposed and developed a proof-of-concept theoretical model of an all-optical transistor where a control beam is used to turn ON and OFF the incoming light. This research reported in this paper makes our optical transistor design unique that would significantly contribute to future all-optical diode design and highly-integrated optical information processing in all-optical integrated chips.